

# A Model-based Genetic Programming Approach for Symbolic Regression of Small Expressions

Marco Virgolin, Tanja Alderliesten, Cees Witteveen, and Peter A.N. Bosman

Submitted to IEEE Transactions on Evolutionary Computation

**Abstract**—The Gene-pool Optimal Mixing Evolutionary Algorithm (GOMEA) is a model-based EA framework that has been shown to perform well in several domains, including Genetic Programming (GP). Differently from traditional EAs where variation acts randomly, GOMEA learns a model of interdependencies within the genotype, i.e., the linkage, to estimate what patterns to propagate. In this article, we study the role of Linkage Learning (LL) performed by GOMEA in Symbolic Regression (SR). We show that the non-uniformity in the distribution of the genotype in GP populations negatively biases LL, and propose a method to correct for this. We also propose approaches to improve LL when ephemeral random constants are used. Furthermore, we adapt a scheme of interleaving runs to alleviate the burden of tuning the population size, a crucial parameter for LL, to SR. We run experiments on 10 real-world datasets, enforcing a strict limitation on solution size, to enable interpretability. We find that the new LL method outperforms the standard one, and that GOMEA outperforms both traditional and semantic GP. We also find that the small solutions evolved by GOMEA are competitive with tuned decision trees, making GOMEA a promising new approach to SR.

**Index Terms**—genetic programming, symbolic regression, linkage, GOMEA, machine learning.

## I. INTRODUCTION

**S**YMBOLIC Regression (SR) is the task of finding a function that explains hidden relationships in data, without prior knowledge on the form of such function. Genetic Programming (GP) [1] is particularly suited for SR, as it can generate solutions of arbitrary form using basic functional components.

Much work has been done in GP for SR, proposing novel algorithms [2], [3], [4], hybrids [5], [6], and other forms of enhancement [7], [8]. What is recently receiving a lot of attention is the use of so-called *semantic-aware* operators, which enhance the variation process of GP by considering intermediate solution outputs [9], [10], [11]. The use of semantic-aware operators has proven to enable the discovery of very accurate solutions, but often at the cost of complexity: solution size can range from hundreds to billions of components [9], [12]. These solutions are consequently impossible to interpret, a fact

M. Virgolin is with Centrum Wiskunde & Informatica, Amsterdam, the Netherlands.

T. Alderliesten is with the Department of Radiation Oncology, Amsterdam UMC, University of Amsterdam, Amsterdam, the Netherlands.

C. Witteveen is with Delft University of Technology, Delft, the Netherlands.

P.A.N. Bosman is with Centrum Wiskunde & Informatica and Delft University of Technology, Delft, the Netherlands.

Manuscript received ?; revised ?.

978-1-5386-5541-2/18/\$31.00 ©2018 IEEE

that complicates or even prohibits the use of GP in many real-world applications because many practitioners desire to understand what a solution means before trusting its use [13]. The use of GP to discover uninterpretable solutions can even be considered to be questionable in many domains, as many alternative machine learning algorithms exist that can produce competitive solutions much faster [14].

We therefore focus on SR when GP is forced to generate small-sized solutions, i.e. mathematical expressions consisting of a small number of basic functional components, so that interpretation is feasible. With size limitation, finding accurate solutions is particularly hard. It is not without reason that many effective algorithms work instead by growing solution size, e.g., by iteratively stacking components [11], [15].

A recurring hypothesis in GP literature is that the evolutionary search can be made effective if *salient patterns*, occurring in the representation of solutions (i.e., the genotype), are identified and preserved during variation [16]. It is worth studying if this holds for SR, to find accurate small solutions.

The hypothesis that salient patterns in the genotype can be found and exploited is what motivates the design of Model-Based Evolutionary Algorithms (MBEAs). Among them, the Gene-pool Optimal Mixing Evolutionary Algorithm (GOMEA) is one of the most successful, and has seen applications in different domains: discrete optimization [17], [18], real-valued optimization [19], but also grammatical evolution [20], and, the focus of this article, GP [21], [22]. GOMEA embodies within each generation a model-learning phase, where *linkage*, i.e. the inter-dependency within parts of the genotype, is modeled. During variation, the linkage information is used to propagate genotype patterns.

The GP instance of GOMEA (GP-GOMEA) was first introduced in [21], to efficiently tackle classic benchmark problems of GP, where pure optimization is pursued. The Interleaved Multistart Scheme (IMS) was also proposed, which is a scheme inspired by [23] that starts multiple evolutionary runs of increasing evolutionary resources (e.g., population size), and executes them in an interleaved fashion. The purpose of the IMS is to relieve the user from the need of tuning the population size, which is particularly crucial for MBEAs: the population needs to be big enough for linkage to be effectively modeled, yet small enough to allow efficient search.

GP-GOMEA has also seen a first adaptation to SR, to find small and accurate solutions for a clinical problem where interpretability is important [22]. There, GP-GOMEA was engineered to work for the particular problem, and no analysis of what linkage learning brings to SR was performed. Also, instead of using the IMS, a fixed population size was adopted.

This is because the IMS was originally designed in [21] to help finding solutions that solve synthetic benchmark problems *to optimality*. To successfully deal with SR, the IMS must be adapted to focus on two crucial aspects: promoting solutions that generalize to unseen data, and limiting solution size.

The aim of this article is to understand the role of linkage learning when dealing with SR, and consequently improve GP-GOMEA, to find small and accurate SR solutions. We present two main contributions. First, we propose an improved linkage learning approach, that, differently from the original one, is unbiased w.r.t. the way the population is initialized. We also analyze how linkage learning is influenced by the presence of many different constant values, sampled by Ephemeral Random Constant (ERC) terminals [16], and propose a strategy to handle them. Second, we introduce a new IMS that is designed to deal with SR, and with learning tasks in general.

The structure of this article interleaves methods with the respective experiments, to describe how we improve GP-GOMEA one step at a time. In Section II, we explain how GP-GOMEA and linkage learning work. Before proceeding with the description of the new contributions and experiments, Section III shows general parameter settings and datasets that will be used along the article. In Section IV we present how we improve linkage learning, and how we deal with ERCs. We propose a new IMS for SR in Section VI, and use it in Section VII to benchmark GP-GOMEA with competing algorithms: traditional GP, GP using a state-of-the-art semantic-aware operator, and the very popular decision tree for regression [24]. In our comparison, the GP algorithms are run with a strict limitation on solution size. Lastly, we discuss our findings and draw conclusions in Section VIII.

## II. GENE-POOL OPTIMAL MIXING EVOLUTIONARY ALGORITHM FOR GP

Three main concepts are at the base of (GP-)GOMEA: solution representation (genotype), linkage learning, and linkage-based variation. These components are arranged in a standard outline that encompasses all algorithms of the GOMEA family.

Algorithm 1 shows the outline of GOMEA. As most EAs, GOMEA starts by initializing a population  $P$ , given the desired population size  $p$ . The generational loop is then started and continues until a termination criterion is met, e.g., a limit on the number of generations or evaluations, or a maximum time. Lines 4 to 8 represent a generation. First, the linkage model is learned, which is called Family of Subsets (FOS) (explained in Sec. II-B). Second, each solution  $P_i$  is used to generate an offspring solution  $O_i$  by the variation operator Gene-pool Optimal Mixing (GOM). Last, the offspring replace the parent population. Note the lack of a separate selection operator. This is because GOM performs variation and selection at the same time (see Sec II-C).

For GP-GOMEA, an extra parameter is needed, the tree height  $h$ . This is necessary to determine the representation of solutions, as described in the following Section II-A.

### A. Solution representation in GP-GOMEA

GP-GOMEA uses a modification of the tree-based representation [1]. While typical GP trees can have any shape, GP-

---

### Algorithm 1 Outline of GOMEA

---

```

1 procedure RUNGOMEA( $p$ )
2    $P \leftarrow \text{initializePopulation}(p)$ 
3   while  $\text{terminationCriteriaNotMet}()$  do
4      $F \leftarrow \text{learnFOS}(P)$ 
5      $O \leftarrow \emptyset$ 
6     for  $i \in \{1, \dots, p\}$  do
7        $O_i \leftarrow \text{GOM}(P_i, P, F)$ 
8      $P \leftarrow O$ 

```

---

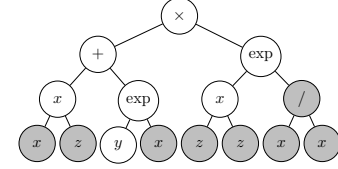


Figure 1. Example of tree for GP-GOMEA with  $h = 3$  and  $r = 2$ . While 15 nodes are present, the nodes that influence the output are only 7: the gray nodes are introns.

GOMEA uses a fixed template, that allows linkage learning and linkage-based variation to be performed in a similar fashion as for other, fixed string-length versions of GOMEA.

All solutions are generated as full  $r$ -ary trees of height  $h$ , with  $r$  being the maximum number of inputs accepted by the functions provided in the function set (e.g., for  $\{+, -, \times\}$ ,  $r = 2$ ), and  $h$  chosen by the user. This is achieved by appending  $r$  child nodes to any node that is not at maximum depth, even if the node is a terminal, or if it is a function requiring less than  $r$  inputs (in this case, the leftmost nodes are used as inputs). Some nodes are thus *introns*, i.e., they are not executed to compute the output of the tree. It follows that, while trees are *syntactically* full, they are not necessarily *semantically* so. All trees of GP-GOMEA have a number of nodes, equal to

$$\ell = \sum_{i=0}^h r^i. \quad (1)$$

Figure 1 shows an example of a tree for GP-GOMEA.

### B. Linkage learning

The linkage model used by GOMEA algorithms is called the Family of Subsets (FOS), and is a set of sets:

$$F = \{F_1, \dots, F_{|F|}\}, F_i \subseteq \{1, \dots, \ell\}.$$

Each  $F_i$  contains indices representing node locations. It is sufficient to choose a parsing order to identify the same node locations in all trees, since trees share the same shape.

In GOMEA, linkage learning corresponds to building a FOS. Different types of FOS exist in literature, however, the by-far most adopted one is the *Linkage Tree* (LT) [25], [21]. The LT captures linkage in hierarchical levels. An LT is typically learned every generation, from the population. To assess whether linkage learning plays a key role, i.e. whether it is better than randomly choosing linkage relations, we also consider the Random Tree (RT) [21].

1) *Linkage Tree*: The LT arranges the sets  $F_i$  in a binary tree structure. The LT uses mutual information as a proxy for linkage strength, as follows. Initially, the leaves of the LT are initialized to singletons  $F_i = \{i\}, \forall i \in \{1, \dots, \ell\}$ . To build the next levels of the LT, mutual information is measured for any pair of genotype locations  $i, j$  in the population, from the distribution of *symbols*. While in a binary genetic algorithm symbols are either ‘0’ or ‘1’, symbols in GP correspond to the

types of function and terminal node, e.g., ‘+’, ‘-’, ‘ $x_1$ ’, ‘ $x_2$ ’. Mutual information between a pair of locations can be computed after measuring entropy for single locations  $H(i)$ , and pairs of locations,  $H(i, j)$ :

$$MI(i, j) = H(i) + H(j) - H(i, j), \quad (2)$$

where

$$H(i) = -\sum P_i \log P_i, \quad H(i, j) = -\sum P_{ij} \log P_{ij}, \quad (3)$$

and  $P_i$  ( $P_{ij}$ ) is the (joint) probability distribution over the symbols at location(s)  $i$  ( $i, j$ ), which can be estimated by counting occurrences in the population genotype.

Once mutual information is computed for all location pairs, the next levels of the LT are built by the clustering algorithm Unweighted Pair Group Method with Arithmetic Mean (UPGMA) [26]. UPGMA only coarsely approximates the real mutual information between higher-order tuples of locations, however it is much faster than calculating mutual information exactly. The LT can be built in  $O(\ell^2 p)$ , and has proven to find higher-order dependencies with sufficient accuracy to efficiently and effectively solve many real-world problems [25]. We remove the root of the LT which corresponds to a set that contains all node locations, and thus provides no linkage information. Thus, the LT contains  $2\ell - 2$  sets.

2) *Random Tree*: While linkage learning assumes an inherent structural inter-dependency to be present within the genotype that can be captured in an LT, such hypothesis may not be true. In such a scenario, using the LT may be not better than building a similar FOS in a completely random fashion. The RT is therefore considered to test this. The RT shares the same tree-like structure of the LT, but is built randomly rather than using mutual information (computational time  $O(\ell)$ ). We use the RT as an alternative FOS for GP-GOMEA.

### C. Gene-pool Optimal Mixing

Once the FOS is learned, the variation operator GOM is used to generate the offspring population. GOM variates a given solution  $P_i$  in iterative steps, by overriding the nodes at the locations specified by each  $F_j$  in the FOS, with the nodes in the same locations taken from random donors in the population. Selection is performed within GOM in a hill-climbing fashion, i.e., variation attempts that result in worse fitness are undone.

The pseudo-code presented in Algorithm 2 describes GOM in detail. To begin, a backup  $B_i$  of the parent solution  $P_i$  is made, including its fitness, and similarly an offspring solution  $O_i = P_i$  is created. Next, the FOS  $F$  is shuffled randomly: this is to provide different combinations of variation steps along the run and prevent bias. For each set of node locations  $F_j$ , a random donor  $D$  is then picked from the population, and  $O_i$  is changed by replacing the nodes specified by  $F_j$  with the homologous ones from  $D$ . It is then assessed whether at least one non-intron node of the tree has been changed by variation (indicated by  $\neq^*$  in line 9). When that is not the case,  $O_i$  will have the same behavior as  $B_i$ , thus the fitness is necessarily identical. Otherwise, the new fitness  $f_{O_i}$  is computed: if not worse than the previous one, the change

is kept, and the backup is updated, otherwise the change is reversed.

Note that if a change results in  $f_{O_i} = f_{B_i}$ , the change is kept. This allows random walks in the neutral fitness landscape [27], [28]. Note also that differently from traditional subtree crossover and subtree mutation [1], GOM can change unconnected nodes at the same time, and keeps tree height limited to the initially specified parameter  $h$ .

---

### Algorithm 2 Pseudocode of GOM

---

```

1 procedure GOM( $P_i, P, F$ )
2    $B_i \leftarrow P_i$ 
3    $f_{B_i} \leftarrow f_{P_i}$ 
4    $O_i \leftarrow P_i$ 
5    $F \leftarrow \text{randomShuffle}(F)$ 
6   for  $F_j \in F$  do
7      $D \leftarrow \text{pickRandomDonor}(P)$ 
8      $O_i \leftarrow \text{overrideNodes}(O_i, D, F_j)$ 
9     if  $O_i \neq^* B_i$  then
10        $f_{O_i} \leftarrow \text{computeFitness}(O_i)$ 
11       if  $f_{O_i} \leq f_{B_i}$  then #Assumption: minimization of f
12          $B_i \leftarrow O_i$ 
13          $f_{B_i} \leftarrow f_{O_i}$ 
14       else
15          $O_i \leftarrow B_i$ 
16          $f_{O_i} \leftarrow f_{B_i}$ 
17     else
18        $B_i \leftarrow O_i$ 

```

---

### III. GENERAL EXPERIMENTAL SETTINGS

We now describe the general parameters that will be used in this article. Table I reports the parameter settings which are typically used in the following experiments, unless specified otherwise. The notation  $\mathbf{x}$  represents the matrix of feature values. We use the Analytic Quotient (AQ) [29] instead of protected division because it has been shown to lead to much better generalization in GP. This is because the AQ is continuous in 0 for the second operand:  $x_1 \div_{\text{AQ}} x_2 := x_1 / \sqrt{1 + x_2^2}$ .

We consider 10 real-world benchmark datasets from literature [12] that can be found on the UCI repository<sup>1</sup> [30] and other sources<sup>2</sup>. The characteristics of the datasets are summarized in Table II.

We use the linearly-scaled Mean Squared Error (MSE) to measure solution fitness [7], as it can be particularly beneficial when evolving small solutions:

$$\text{MSE}(y, \tilde{y}) = \frac{1}{n} \sum_i^n (y_i - (a + b\tilde{y}_i))^2,$$

where  $y_i$  is the value of the variable to regress for the  $i$ th example, and  $\tilde{y}_i$  the respective solution prediction. The constants  $a$  and  $b$  can be calculated in  $O(n)$  with:

$$a = \mu(y) - b\mu(\tilde{y}),$$

$$b = \sum_i^n \frac{(y_i - \mu(y))(\tilde{y}_i - \mu(\tilde{y}))}{(\tilde{y}_i - \mu(\tilde{y}))^2},$$

with  $\mu$  computing the mean. We present our results in terms of variance-Normalized MSE (NMSE), i.e.  $\frac{\text{MSE}(y, \tilde{y})}{\text{var}(y)}$ , so that results from different datasets are on a similar scale.

To assess statistical significance when comparing two algorithms (or configurations) on a certain dataset, we use the

<sup>1</sup><https://archive.ics.uci.edu/ml/index.php>

<sup>2</sup><https://goo.gl/tn6Zxv>

Table I  
GENERAL PARAMETER SETTINGS FOR THE EXPERIMENTS

Parameter	Setting
Function set	$\{+, -, \times, \div, \text{AQ}\}$
Terminal set	$\mathbf{x} \cup \{\text{ERC}\}$
ERC bounds	$[\min \mathbf{x}, \max \mathbf{x}]$
Initialization for GP-GOMEA	Half-and-Half as in [22]
Tree height $h$	4
Train-validation-test split	50%–25%–25%
Experiment repetitions	30

Table II  
REGRESSION DATASETS USED IN THIS WORK

Name	Abbreviation	# Features	# Examples
Airfoil	Air	5	1503
Boston housing	Bos	13	506
Concrete compres. str.	Con	8	1030
Dow chemical	Dow	57	1066
Energy cooling	EnC	8	768
Energy heating	EnH	8	768
Tower	Tow	25	4999
Wine red	WiR	11	1599
Wine white	WiW	11	4898
Yacht hydrodynamics	Yac	6	308

Wilcoxon signed-rank test [31], paired by random seed. The seed determines the particular split of the examples between training, validation, and test sets, and also the sampling of the initial population. We consider a difference to be significant if a smaller  $p$ -value than 0.05 is found. We also apply the Holm-Bonferroni method [32], to prevent false positives. If more than two algorithms need to be compared, we first perform a Friedman test on mean performance over all datasets [31]. We use the symbols  $\blacktriangle$ ,  $\blacktriangledown$  to respectively indicate significant superiority, and inferiority (absence of a symbol means no significant difference). The result *next* to the symbol  $\blacktriangle$  ( $\blacktriangledown$ ) signifies a result being better (worse) than the result obtained by the algorithm that has the same color of the symbol. Algorithms and/or configurations are color coded in each table reporting results (colors are color-blind safe).

Our code (in C++) can be found at: <https://goo.gl/15tMV7>.

#### IV. IMPROVING LINKAGE LEARNING FOR GP

In previous work on GP-GOMEA, learning the LT was performed the same way it is done for any discrete GOMEA implementation, i.e. by computing the mutual information between pairs of locations  $(i, j)$  in the genotype (Eq. 2) [21]. However, the distribution of node types is typically not uniform when a GP population is initialized (e.g., function nodes never appear as leaves). In fact, it depends on the cardinality of the function and terminal sets, and on the population initialization method, (e.g., *Full*, *Grow*, *Half-and-Half*, *Ramped Half-and-Half* [33]). This lack of uniformity leads to an imbalance in mutual information, suggesting the presence of linkage. However, it is reasonable to expect no linkage to be present in an initialized population, as evolution did not take place yet.

Figure 2 (left) shows the mutual information matrix between pairs of node locations in an initial population of 1,000,000 solutions with maximum height  $h = 2$ , using *Half-and-Half*,

a function set of size 4 with maximum number of inputs  $r = 2$ , and a terminal set of size 6 (no ERCs are used). Each tree contains exactly 7 nodes (Eq. 1). We index node locations with pre-order tree traversal, i.e., 1 is the root, 2 its first child, 5 its second child, 3, 4 are (leaves) children of 1, and 6, 7 are (leaves) children of 5. It can be seen that the mutual information matrix of location pairs falsely suggests the existence of linkage (e.g., larger mutual information values are present between non-leaf nodes).

We hypothesize that, if we correct linkage learning so that no patterns emerge at initialization, the truly salient patterns will have a bigger chance of emerging during evolution, and better results will be achieved. We now discuss how such a correction can be performed.

##### A. Not uniform sampling and mutual information

A possibility to overcome the aforementioned problem is to modify the mutual information to take into account the non-uniformity of the distribution of node types in the initial population. Since mutual information depends on entropy (Eq. 2 and 3), we can attempt to normalize the entropy.

We begin by considering the fact that, in principle, symbols at a specific location  $i$  can be sampled by a location-specific set  $\Omega_i$ . For example, in GP, tree leaves are necessarily terminal nodes. For brevity, we now focus on univariate entropy  $H(i)$ , but similar considerations hold for the joint entropy  $H(i, j)$ . We rewrite Eq. 3 as:

$$H(i) = - \sum_{\omega \in \Omega_i} P_i(\omega) \log P_i(\omega).$$

A normalized entropy is then given by using a proper base  $b_i$  for the logarithm. Under normal circumstances, it suffices to set  $b_i = |\Omega_i|$ .

For an initial population of GP, several issues are present. For a location  $i$ ,  $\Omega_i$  is typically not fixed, rather it depends on the probability that the function or the terminal set is used to sample nodes at that location (e.g., due to using the Ramped Half-and-Half initialization method). Even if  $b_i$  can be exactly determined, locations  $i, j, i \neq j$  may have different a priori probability distributions  $P_i \neq P_j$ , thus resulting in  $H(i) \neq H(j)$ , and therefore introducing linkage learning bias. Thus, we propose a simple approximation method.

##### B. Sample-based normalization of mutual information

Let us consider the case where a correct logarithm base  $b$  is used (we now drop the subscript  $i$  from  $b_i$  for the sake of readability), and symbols in each location are distributed uniformly. We get  $H_b(i) = 1$ ,  $H_b(i, j) = 2$  for  $i \neq j$ , and  $H_b(i, j) = 1$  for  $i = j$ . The mutual information must then be (Eq. 2):

$$\text{MI}_b(i, j) = 1 + 1 - 2 = 0 \text{ for } i \neq j, \text{ else } 1,$$

i.e. the identity matrix  $I$ .

Now, consider that  $H_b$  can be written as:

$$\begin{aligned} H_b(i) &= - \sum P_i \log_b P_i = - \sum P_i \frac{\log P_i}{\log b} = \\ &= - \frac{1}{\log b} \sum P_i \log P_i = \frac{1}{\log b} H(i). \end{aligned}$$

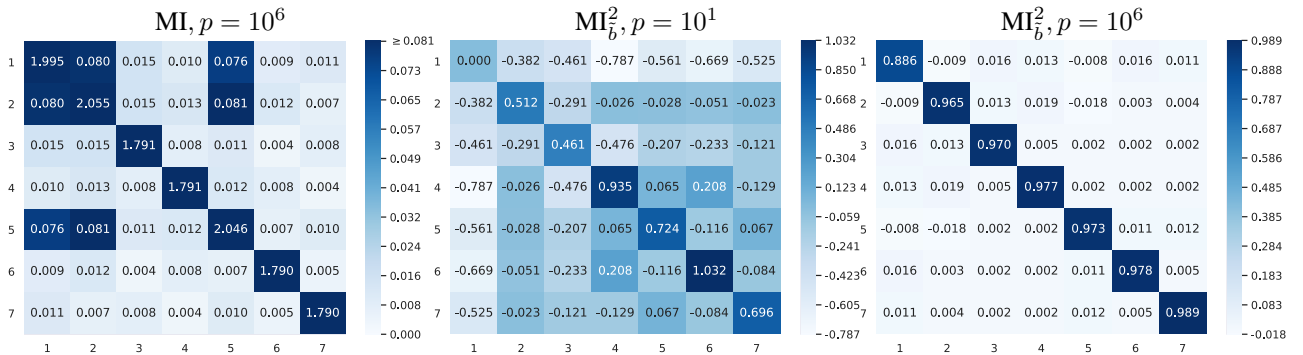


Figure 2. Mutual information matrix between pairs of locations in the genotype (x and y labels). Darker blue represents higher values. Left: Matrix for an initialized population of size  $10^6$ . The values suggest the existence of linkage even though no evolution has taken place yet. Middle and Right: Mutual information matrices at the second generation using our normalization method, with population size of 10 (middle), and of  $10^6$  (right) for a particular run of GP-GOMEA. The rightmost matrix is closest to the identity  $I$ .

This means we need to determine  $\frac{1}{\log b} =: \beta_i$  to transform  $H(i)$  into  $H_b(i)$ . We now make the assumption that the initial population sample is sufficiently representative of the true distribution of nodes. We want the initial population to have  $H_b^{\text{init}}(i) = 1$ , and  $H_b^{\text{init}}(i, j) = 2$ . For this, it suffices to set:

$$\beta_i = \frac{1}{H^{\text{init}}(i)}, \beta_{i,j} = \frac{2}{H^{\text{init}}(i, j)}.$$

Thus, we simply compute the  $\beta$  coefficients for the initial population, and then use them during the linkage learning phase (i.e., to build the LT) each generation. The mutual information computed at generation  $g$  will then be:

$$MI_{\tilde{b}}^g(i, j) = \beta_i H^g(i) + \beta_j H^g(j) - \beta_{i,j} H^g(i, j). \quad (4)$$

The tilde in  $\tilde{b}$  is to remark that this is an approximation.

### C. Approximation error of $MI_{\tilde{b}}$

As a preliminary step, we observe the error associated with using the approximately normalized mutual information  $MI_{\tilde{b}}$ . To have a crude estimate of the approximation error, we report a typical mutual information matrix computed at the second generation of a GP-GOMEA run on the dataset Yac (at the first one  $MI_{\tilde{b}}^1 = I$  by construction). We repeat this for two population sizes,  $p = 10$  and  $p = 1,000,000$ . We expect that, the bigger  $p$ , the lower the approximation error.

We use the parameters of Table I, a terminal set of size 6 (the features of Yac, no ERC) and  $h = 2$ , i.e.  $\ell = 7$  nodes per tree. Figure 2 (middle and right) shows the mutual information matrix between location pairs, for the two population sizes. It can be seen that the values can erroneously be lower than 0 or bigger than 1. However, while this is particularly marked for  $p = 10$ , with minimum of -0.787 and maximum of 1.032, it becomes less evident for  $p = 10^6$ , with minimum of -0.018 and maximum of 0.989. The fact that  $MI_{\tilde{b}}^2 \approx I$  for  $p = 10^6$  is because, with such a large population size, a lot of diversity is still present in the second generation.

### D. Experiment: $LT-MI_{\tilde{b}}$ vs $LT-MI$ vs RT

We now test the use of  $MI_{\tilde{b}}$  over the standard MI for GP-GOMEA with the LT. We use the notation  $LT-MI_{\tilde{b}}$  and  $LT-MI$  to refer to the two configurations. We further consider the RT

to see if using mutual information to drive variation is any better than random.

We set the population size to 2000 as a compromise between having enough samples for linkage to be learned, and meeting typical literature values, which range from hundreds to a few thousands. We use the function set of Table I, and a tree height  $h = 4$  (thus  $\ell = 31$ ). We set a limit of 20 generations, which is approximately equivalent to 1200 generations of traditional GP, since each solution is evaluated up to  $2\ell - 2$  times (size of the LT minus non-meaningful changes, see Sec. II-B and Sec. II-C).

### E. Results: $LT-MI_{\tilde{b}}$ vs $LT-MI$ vs RT

The training and test NMSE performances are reported in Table III. The Friedman test results in significant differences along training and test performance. GP-GOMEA with  $LT-MI_{\tilde{b}}$  is clearly the best performing algorithm, with significantly lower NMSE compared to  $LT-MI$  on 8/10 datasets when training, and 7/10 at test time. It is always better than using the RT when training, and in 9/10 cases when testing. The  $LT-MI$  is comparable with the RT.

The result of this experiment is that the use of the new  $MI_{\tilde{b}}$  to build the LT simply enables GP-GOMEA to perform a more competent variation than the use of MI. Also, using the LT this way leads to better results than when making random changes with the RT. Figure 3 shows the evolution of the training NMSE for the dataset Yac. It can be seen that the  $LT-MI_{\tilde{b}}$  allows to quickly reach smaller errors than the other two FOS types. We observed similar training patterns for the other datasets (not shown here).

In the remainder, when we write “LT”, we refer to  $LT-MI_{\tilde{b}}$ .

### F. Experiment: impact of pattern propagation

The previous experiment showed that using linkage-driven variation (LT) can be favorable compared to random variation (RT). This result seems to confirm the hypothesis that, in certain SR problems, salient underlying patterns in the genotype exist that can be exploited.

Another aspect is how final solutions look: if linkage learning identifies specific patterns, it can be reasonably expected

Table III

RESULTS OF LINKAGE LEARNING WITH CORRECTION OF MUTUAL INFORMATION: MEDIAN NMSE OF 30 RUNS FOR GP-GOMEA WITH LT-MI $_{\tilde{b}}$ , LT-MI, AND RT.

Dataset	Training			Test		
	LT-MI $_{\tilde{b}}$	LT-MI	RT	LT-MI $_{\tilde{b}}$	LT-MI	RT
Air	29.9 $\blacktriangle$	31.2 $\blacktriangledown$	32.7 $\blacktriangledown$	31.8 $\blacktriangle$	34.8 $\blacktriangledown$	34.0 $\blacktriangledown$
Bos	15.4 $\blacktriangle$	15.4 $\blacktriangledown$	17.5 $\blacktriangledown$	24.0 $\blacktriangledown$	23.0 $\blacktriangle$	22.5 $\blacktriangle$
Con	17.5 $\blacktriangle$	18.5 $\blacktriangledown$	19.0 $\blacktriangledown$	18.7 $\blacktriangle$	19.6 $\blacktriangledown$	20.1 $\blacktriangledown$
Dow	20.9 $\blacktriangledown$	20.3 $\blacktriangle$	24.0 $\blacktriangledown$	22.6 $\blacktriangledown$	21.1 $\blacktriangle$	26.0 $\blacktriangledown$
Enc	8.4 $\blacktriangle$	9.7 $\blacktriangledown$	9.1 $\blacktriangledown$	9.2 $\blacktriangle$	10.7 $\blacktriangledown$	10.3 $\blacktriangle$
EnH	6.2 $\blacktriangle$	6.4 $\blacktriangledown$	6.4 $\blacktriangle$	6.5 $\blacktriangle$	7.1 $\blacktriangledown$	6.7 $\blacktriangle$
Tow	12.5 $\blacktriangledown$	12.5 $\blacktriangle$	13.1 $\blacktriangledown$	13.0 $\blacktriangle$	12.8 $\blacktriangle$	13.2 $\blacktriangledown$
WiR	60.3 $\blacktriangle$	60.9 $\blacktriangledown$	61.2 $\blacktriangledown$	62.5 $\blacktriangle$	63.0 $\blacktriangledown$	63.1 $\blacktriangledown$
WiW	68.1 $\blacktriangle$	68.4 $\blacktriangledown$	68.7 $\blacktriangledown$	69.1 $\blacktriangle$	69.7 $\blacktriangledown$	69.5 $\blacktriangle$
Yac	0.3 $\blacktriangle$	0.4 $\blacktriangledown$	0.4 $\blacktriangledown$	0.6 $\blacktriangle$	0.6 $\blacktriangledown$	0.6 $\blacktriangledown$

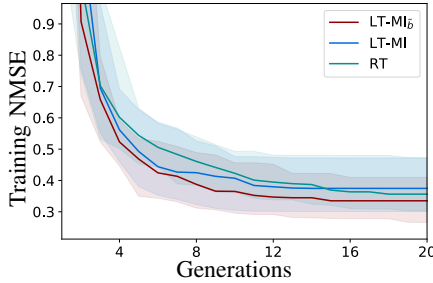


Figure 3. Median fitness of the best solution of 30 runs on Yac, for LT-MI $_{\tilde{b}}$ , LT-MI, and RT (10<sup>th</sup> and 90<sup>th</sup> percentiles in shaded area).

that their propagation will lead to the discovery of similar solutions over different runs.

Therefore, we now want to assess whether the use of the LT has a bigger chance to lead to the discovery of a particular solution, compared to the use of the RT. We use the same parameter setting as described in Sec. IV-D, but perform 100 repetitions. While each run uses a different random seed (e.g., for population initialization), we fix the dataset split, as changing the training set results in changing the fitness function. We repeat the 100 runs on 5 random dataset splits, on the smallest dataset Yac. Together with  $p = 2000$  as in the previous experiment, we also consider a doubled  $p = 4000$ .

#### G. Results: impact of pattern propagation

Table IV reports the number of solutions that have at least one duplicate, i.e. their genotype is semantically equivalent (e.g.,  $x_1 + x_2 = x_2 + x_1$ ), along different runs for 5 random splits of Yac. It can be seen that the LT finds more duplicate solutions than the RT, by a margin of around 30%.

Figure 4 shows the distribution of solutions found for the second dataset split with  $p = 4000$ , i.e. where both the LT and the RT found a large number of duplicates. The LT has a marked chance of leading to the discovery of a particular solution, up to one-fourth of the times. When the RT is used, a same solution is found only up to 6 times out of 100.

This confirms the hypothesis that linkage-based variation can propagate salient patterns more than random variation should such patterns exist, enhancing the likelihood of discovering particular solutions.

#### V. EPHEMERAL RANDOM CONSTANTS & LINKAGE

In many GP problems, and in particular in SR, the use of ERCs can be very beneficial [16]. An ERC is a special

Table IV

PERCENTAGE OF BEST SOLUTIONS WITH DUPLICATES FOUND BY GP-GOMEA WITH LT AND RT FOR DIFFERENT SPLITS OF YAC.

Split	$p = 2000$		$p = 4000$	
	LT	RT	LT	RT
1	36	18	44	15
2	42	12	49	21
3	40	7	43	8
4	43	8	45	25
5	36	16	49	16
Avg.	39	12	46	17

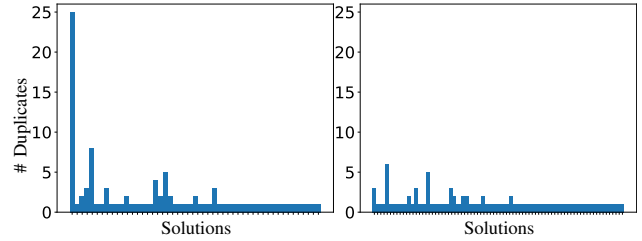


Figure 4. Distribution of solutions found for 100 runs by using the LT (left) and the RT (right) with  $p = 4000$  on the second dataset split of Yac.

terminal which is set to a constant only when instantiated in a solution. In SR, this constant is commonly sampled uniformly at random from a user-defined interval.

Because every node instance of ERC is a different constant, linkage learning needs to deal with a large number of different symbols. This can lead to two shortcomings. First, a very large population size may be needed for salient patterns to emerge. Second, data structures used to store the frequencies of symbols grow really big and become slow (e.g., hash maps).

We explore three strategies to deal with this:

- 1) all-const: Ignore the shortcomings, and consider all different constants as different symbols during linkage learning.
- 2) no-const: Skip all constants during linkage learning, i.e. set their frequency to zero. This approximation is reasonable since all constants are unique at initialization, and the respective frequency is almost zero. However, during evolution some constants will be propagated while others will be discarded, making this approximation less and less accurate over time.
- 3) bin-const: Perform on-line binning. We set a maximum number  $\gamma$  of constants to consider. After  $\gamma$  different constants have been encountered in frequency counting, any further constant is considered to fall into the same bin as the closest constant among the first  $\gamma$ . The closest constant can be determined with binary search in  $\log_2(\gamma)$  steps. Contrary to strategy no-const, the error of this approximation lowers over time, as less useful constants get discarded during evolution.

#### A. Experiment: linkage learning with ERCs

We use the same parameter setup of the experiment in Sec. IV-D, this time adding an ERC terminal to the terminal set. We compare the three strategies to handle ERCs when learning the LT. For this experiment and in the rest of the article, we use  $\gamma = 100$  in bin-const. We observed that

for problems with a small number of features (e.g., Air and Yac), i.e., where ERC sampling is more likely and thus more constants are produced, this choice reduces the number of constant symbols to be considered by linkage learning in the first generations by a factor of  $\sim 50$ . We also report the results obtained with the RT as a baseline, under the hypothesis that using ERCs compromises linkage learning to the point that random variation becomes equally good or better.

### B. Results: linkage learning with ERCs

The results of this experiment are shown in Table V, including the time taken to complete 20 generations. The Friedman test reveals significant differences among the configurations for train, test, and time performance. Note that the use of ERCs leads to lower errors compared to not using them (compare with Table III).

In terms of training error, the RT is always outperformed by the use of the LT, no matter the strategy. The all-const strategy is significantly better than no-const in half of the problems, and never worse. Overall, bin-const performs best, with 6 out of 10 significantly better results than all-const. The fact that all-const can be outperformed by bin-const supports the hypothesis that linkage learning can be compromised by the presence of too many constants to consider, which hide the true salient patterns. Test results are overall similar to the training ones, but less comparisons are significant.

In terms of time, all-const is almost always significantly worse than the other methods, and often by a consistent margin. This is particularly marked for problems with a small number of features (i.e., Air, Yac). There, more random constants are present in the initial population, since the probability of sampling the ERC from the terminal set is inversely proportional to the number of features.

Interestingly, despite the lack of a linkage-learning overhead, using the RT is not always the fastest option. This is because random variation leads to a slower convergence of the population compared to the linkage-based one, where salient patterns are quickly propagated, and less variation attempts result in changes of the genotype that require a fitness evaluation (see Sec. II-C). The slower convergence caused by the RT can also be seen in Figure 3 (for the previous experiment), and was also observed in other work, in terms of diversity preservation [34].

Between the LT-based strategies, the fastest is no-const, at the cost of a bigger training error. Although consistently slower than no-const, bin-const is still quite fast, and achieves the lowest training errors. We found bin-const to be preferable in test NMSE as well. In the following, we always use bin-const, with  $\gamma = 100$ .

## VI. INTERLAVED MULTISTART SCHEME

The Interleaved Multistart Scheme (IMS) is a wrapper for evolutionary runs largely inspired by the work of [23] on genetic algorithms. It works by interleaving the execution of several runs of increasing resources (e.g., population size), each performing one generation only after  $g$  generations of the run with one level less of computational resources ( $g \geq 2$ ).

The main motivation for using the IMS is to make an EA much more robust to parameter selection, and alleviate the need for practitioners to tinker with parameters. The IMS or similar schemes are often used with MBEAs [35], [36], where population size plays a crucial role in determining the quality of model building.

An IMS for GP-GOMEA was first proposed in [21], and its outline is as follows. A collection  $\sigma_{\text{base}}$  is given as input, which is a collection of base parameter settings that will be used in the first run. The IMS runs until a termination criteria is met (e.g., number of generations, time budget). A certain run  $R_i$  performs one generation if no previous runs exist ( $i = 1$  or all previous run have been terminated), or if the previous run  $R_{i-1}$  executed  $g$  generations. The first time  $R_i$  is about to execute a generation, it is initialized, using the run index  $i$  to determine how to scale the base parameters  $\sigma_{\text{base}}$ . For example, the population size can be set to  $2^{i-1}p_{\text{base}}$  (i.e., doubling the population size of the previous run). Finally, a check is done to determine if the run should be terminated (explained below).

### A. Adapting the IMS to learning tasks

The first implementation of the IMS for GP-GOMEA was designed to deal with GP benchmark problems of pure optimization. Such implementation works as follows:

- 1) Scaling parameters — The scaling parameters are population size and tree height. The base population size scales with  $p_i = 2^{i-1}p_{\text{base}}$ , with  $i$  the index of run  $R_i$ . The tree height scales with  $h_i = h_{\text{base}} + \lfloor \frac{i}{2} \rfloor$ .
- 2) Termination — A run  $R_i$  is terminated if the mean population fitness is worse than the one of a subsequent run  $R_j$ ,  $j > i$ , or if it converges to all identical solutions. All smaller runs  $R_k$ ,  $k < i$  are terminated as well.

Scaling the tree height was originally implemented to ensure that solutions will eventually be large enough to accommodate all necessary symbols to find the optimum for benchmark problems [21]. However, in SR and in general learning tasks, no optimum is known beforehand, and it is rather desired to find a solution that generalizes well to unseen examples. Thus, we remove the scaling of  $h$  from the IMS (only  $p$  scales). This is also motivated by the fact that  $h$  bounds the maximum solution size, which then plays a role in interpretability. We leave  $h$  as a parameter for the user to decide, and, if interpretability is sought for, we recommend to use small values for it, e.g.,  $\leq 4$  (see Sec. VIII).

We then change the run termination criteria. In SR, it can happen that the error of a few solutions becomes extremely big, compromising the mean population fitness. This can trigger the termination criteria even if solutions exist that are competitive with the ones of other runs. For this reason, we now consider the fitness of the best solution rather than the mean population fitness. Also different from the first version of the IMS, when terminating a run, we do not automatically terminate all previous runs. Indeed, some smaller runs may still be very competitive (e.g., due to the fortunate sampling of particular constants when using ERCs).

We lastly propose to exploit the fact that many runs are performed within the IMS to tackle a central problem of

Table V  
RESULTS OF LINKAGE LEARNING WITH ERCs: MEDIAN TRAINING NMSE AND MEDIAN TIME OF 30 RUNS FOR GP-GOMEA WITH THE LT USING THE THREE STRATEGIES ALL-CONST, NO-CONST, BIN-CONST, AND WITH THE RT.

Dataset	Training NMSE				Test NMSE				Time (s)			
	all-const	no-const	bin-const	RT	all-const	no-const	bin-const	RT	all-const	no-const	bin-const	RT
Air	27.7	28.0	27.5	31.4	28.7	29.6	27.8	32.5	355.4	71.4	80.0	80.1
Bos	15.2	15.3	15.0	17.6	24.2	23.2	21.8	24.2	63.4	29.4	30.9	24.5
Con	17.2	17.2	17.0	18.5	18.5	18.7	18.8	19.8	154.9	56.7	59.8	58.4
Dow	21.4	21.1	20.7	24.5	22.8	21.9	22.5	25.5	53.8	51.7	54.9	37.7
EnC	5.5	5.7	5.8	6.4	6.2	6.3	6.0	6.8	147.2	40.5	43.5	45.6
EnH	3.0	3.1	2.8	4.1	3.3	3.3	3.1	4.7	145.0	45.8	49.4	45.7
Tow	12.3	12.2	12.3	13.2	12.9	12.8	12.8	13.5	255.9	246.6	245.6	233.9
WiR	60.3	60.2	60.2	61.2	63.6	62.9	62.9	63.2	126.1	67.7	80.2	70.1
WiW	67.6	68.1	68.0	68.5	68.9	69.0	69.4	69.9	285.0	213.3	237.2	224.1
Yac	0.3	0.3	0.3	0.4	0.6	0.6	0.5	0.6	236.5	23.9	24.8	22.8

learning tasks: generalization. Instead of discarding the best solutions of terminating runs, we store them in an archive. When the IMS terminates, we re-compute the fitness of each solution in the archive using a set of examples different from the training set, i.e. the validation set, and return the new best performing, i.e., the solution that generalized best. The final test performance is measured on a third, separate set of examples (test set).

## VII. BENCHMARKING GP-GOMEA

We compare GP-GOMEA (using the new LT) with Tree-based GP with traditional subtree crossover and subtree mutation (GP-Trad), tree-based GP using the state-of-the-art, semantic-aware operator Random Desired Operator (GP-RDO) [9], and Decision Tree for Regression (DTR) [24]. We consider DTR as a state-of-the-art algorithm in delivering interpretable models [37]. We remark that DTR ensembles (e.g., [38], [15]) are typically markedly more accurate than single DTRs, but can quickly become uninterpretable.

### A. Experimental setup

For the EAs, we use a fixed time limit of 1,000 seconds<sup>3</sup>, so that the time taken by GP-GOMEA to learn the LT is taken into account. We consider maximum solution sizes  $l$  of 31 nodes, i.e.  $h = 4$  for GP-GOMEA, as we found that interpretation of the resulting solutions can then already be considered difficult in some cases. The EAs are run with a typical fixed population size  $p = 1000$  (if the population of GP-GOMEA converges, it is randomly re-started), and also with the IMS, considering three values for the number of subgenerations  $g$ : 4, 6, and 8. Choices of  $g$  between 4 and 8 are standards from literature [19], [21], [23].

Our implementation of GP-Trad and GP-RDO mostly follows the one of [9]. The population is initialized with the *Ramped Half-and-Half* method, with tree height between 2 and  $h$ . Selection is performed with tournament of size 7. GP-Trad uses a rate of 0.9 for subtree crossover, and of 0.1 for subtree mutation. GP-RDO uses the population-based library of subtrees, a rate of 0.9 for RDO, and of 0.1 for subtree mutation. Subtree roots to be variated are chosen with the *uniform depth mutation* method, which makes nodes of all depths equally likely to be selected [9]. Elitism is ensured by cloning the best solution into the next generation.

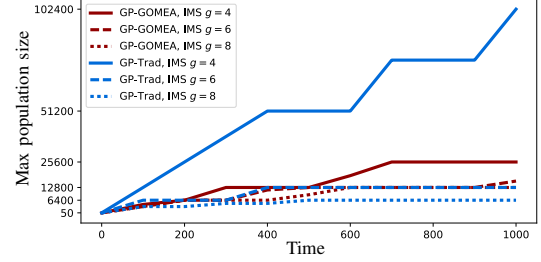


Figure 5. Maximum population size reached (vertical axis) in time (seconds, horizontal axis) with the IMS for GP-GOMEA and GP-Trad, for  $g \in \{4, 6, 8\}$ . The median among problems and repetitions is shown.

We set the maximum solution size for GP-Trad and GP-RDO to 31, i.e. the same limit imposed by  $h = 4$  to GP-GOMEA. Note that a solution size limit rather than a tree height limit allows more freedom in evolving the shape of trees, which has been shown to be beneficial in literature [39], [40]. We also observed this in preliminary experiments.

We use the Python Scikit-learn implementation of DTR [41], with 5-fold cross-validation grid-search over the training set to tune the following hyper-parameters:  $\text{splitter} \in \{\text{'best'}, \text{'random'}\}$ ;  $\text{max\_features} \in \{\frac{1}{2}, \frac{3}{4}, 1\}$ ;  $\text{max\_depth} \in \{3, 4, 5, 6\}$  (documentation available at <http://goo.gl/hbyFq2>). The best generalizing model found by cross-validation is then used on the test set.

### B. Results: benchmarking GP-GOMEA

We consider validation and test NMSE. We now show validation rather than training error because the IMS returns the solution which better generalizes to the validation set among the ones found by different runs (same for DTR due to cross-validation). Use of the Friedman test reveals significant differences among the algorithms. As we are only interested in benchmarking GP-GOMEA, we test whether significant performance differences exist only between GP-GOMEA and the other algorithms.

Table VI shows the NMSE of the algorithms on the validation set, together with the outcomes of the Wilcoxon signed-rank test. We first compare GP-GOMEA with GP-Trad, for the traditional  $p = 1000$ . In this case, no EA can be preferred, in that each one is significantly better than the other one for three different problems. Here, GP-GOMEA does not outperform GP-Trad possibly because the population size is too small for linkage learning to be effective.

<sup>3</sup>Experiments were run on an Intel® Xeon® Processor E5-2650 v2.

Table VI

MEDIAN VALIDATION NMSE OF 30 RUNS FOR GP-GOMEA (GOM), GP-TRAD (TRA), GP-RDO (RDO) WITH  $p = 1000$  AND IMS WITH  $g \in \{4, 6, 8\}$ , AND DTR. SIGNIFICANCE IS ASSESSED WITHIN EACH POPULATION SCHEME W.R.T. GP-GOMEA. THE LAST ROW REPORTS THE NUMBER OF TIMES THE EA PERFORMS SIGNIFICANTLY BETTER (B) AND WORSE (W) THAN GP-GOMEA.

Dataset	$p = 1000$			IMS $g = 4$			IMS $g = 6$			IMS $g = 8$			
	GOM	TRA	RDO	GOM	TRA	RDO	GOM	TRA	RDO	GOM	TRA	RDO	DTR
Air	26.3	32.2 $\blacktriangledown$	35.9 $\blacktriangledown$	24.7	22.9 $\blacktriangle$	37.1 $\blacktriangledown$	24.4	24.9 $\blacktriangledown$	37.9 $\blacktriangledown$	24.4	24.8	36.8 $\blacktriangledown$	30.8 $\blacktriangledown$
Bos	22.3	19.3	24.0 $\blacktriangledown$	16.7	16.0 $\blacktriangledown$	19.7 $\blacktriangledown$	16.5	17.1 $\blacktriangledown$	20.2 $\blacktriangledown$	17.0	17.0 $\blacktriangledown$	20.1 $\blacktriangledown$	22.7 $\blacktriangledown$
Con	17.5	18.5 $\blacktriangledown$	21.3 $\blacktriangledown$	16.6	17.3	20.8 $\blacktriangledown$	17.0	17.6 $\blacktriangledown$	20.5 $\blacktriangledown$	16.6	16.9 $\blacktriangledown$	20.4 $\blacktriangledown$	22.8 $\blacktriangledown$
Dow	20.9	22.2	24.0 $\blacktriangledown$	19.0	19.1	25.6 $\blacktriangledown$	19.4	19.9 $\blacktriangledown$	25.0 $\blacktriangledown$	19.5	19.9 $\blacktriangledown$	25.6 $\blacktriangledown$	30.6 $\blacktriangledown$
EnC	5.3	5.2 $\blacktriangle$	7.3 $\blacktriangledown$	4.7	4.9 $\blacktriangledown$	7.2 $\blacktriangledown$	4.7	4.6 $\blacktriangledown$	8.8 $\blacktriangledown$	4.4	4.9 $\blacktriangledown$	7.8 $\blacktriangledown$	4.1 $\blacktriangle$
EnH	2.3	1.8 $\blacktriangle$	6.0 $\blacktriangledown$	2.0	1.5 $\blacktriangle$	5.0 $\blacktriangledown$	2.0	1.6 $\blacktriangle$	6.1 $\blacktriangledown$	1.9	1.6	5.7 $\blacktriangledown$	0.4 $\blacktriangle$
Tow	12.0	12.7 $\blacktriangledown$	17.7 $\blacktriangledown$	11.9	12.0 $\blacktriangledown$	18.2 $\blacktriangledown$	12.1	12.2 $\blacktriangledown$	16.6 $\blacktriangledown$	12.0	11.9 $\blacktriangledown$	17.4 $\blacktriangledown$	11.1 $\blacktriangle$
WiR	64.3	64.6	66.0 $\blacktriangledown$	63.2	62.8	64.5 $\blacktriangledown$	62.8	62.9	64.8 $\blacktriangledown$	62.8	62.2	64.8 $\blacktriangledown$	71.5 $\blacktriangledown$
WiW	70.1	70.2	71.0 $\blacktriangledown$	69.6	69.7	70.9 $\blacktriangledown$	69.3	69.7	70.4 $\blacktriangledown$	69.8	69.3	71.1 $\blacktriangledown$	72.2 $\blacktriangledown$
Yac	0.5	0.5 $\blacktriangle$	0.6 $\blacktriangledown$	0.4	0.4 $\blacktriangledown$	0.6 $\blacktriangledown$	0.4	0.4	0.5 $\blacktriangledown$	0.4	0.4 $\blacktriangledown$	0.6 $\blacktriangledown$	0.9 $\blacktriangledown$
B/W	—	3/3	0/10	—	2/4	0/10	—	1/6	0/10	—	0/6	0/10	3/7

Table VII  
MEDIAN TEST NMSE, DETAILS AS IN TABLE VI.

Dataset	$n_{\text{pop}} = 1000$			IMS $g = 4$			IMS $g = 6$			IMS $g = 8$			
	GOM	TRA	RDO	GOM	TRA	RDO	GOM	TRA	RDO	GOM	TRA	RDO	DTR
Air	26.4	30.3 $\blacktriangledown$	37.2 $\blacktriangledown$	26.1	23.7 $\blacktriangle$	37.4 $\blacktriangledown$	25.1	25.3	39.5 $\blacktriangledown$	25.0	26.1	39.1 $\blacktriangledown$	31.2 $\blacktriangledown$
Bos	20.8	20.9 $\blacktriangledown$	26.4 $\blacktriangledown$	18.8	21.3 $\blacktriangledown$	22.8 $\blacktriangledown$	20.4	21.5 $\blacktriangledown$	22.7 $\blacktriangledown$	20.0	21.4 $\blacktriangledown$	24.4 $\blacktriangledown$	25.5 $\blacktriangledown$
Con	17.4	17.7 $\blacktriangledown$	21.6 $\blacktriangledown$	16.9	17.1 $\blacktriangledown$	21.6 $\blacktriangledown$	16.6	16.9	21.0 $\blacktriangledown$	17.1	16.9	20.5 $\blacktriangledown$	21.3 $\blacktriangledown$
Dow	19.9	22.4 $\blacktriangledown$	23.9 $\blacktriangledown$	19.1	18.7	24.0 $\blacktriangledown$	18.8	18.4	23.7 $\blacktriangledown$	18.5	20.1 $\blacktriangledown$	25.2 $\blacktriangledown$	27.6 $\blacktriangledown$
EnC	5.3	5.0 $\blacktriangle$	6.9 $\blacktriangledown$	4.4	4.8	7.5 $\blacktriangledown$	4.5	4.8	9.3 $\blacktriangledown$	4.7	4.8 $\blacktriangledown$	8.0 $\blacktriangledown$	4.6 $\blacktriangle$
EnH	2.2	1.9 $\blacktriangle$	5.4 $\blacktriangledown$	2.1	1.6 $\blacktriangle$	5.3 $\blacktriangledown$	2.1	1.8 $\blacktriangle$	5.5 $\blacktriangledown$	2.0	1.5	5.8 $\blacktriangledown$	0.3 $\blacktriangle$
Tow	11.8	13.0 $\blacktriangledown$	18.2 $\blacktriangledown$	11.9	12.0	18.6 $\blacktriangledown$	11.9	12.1	16.7 $\blacktriangledown$	11.8	12.0	16.9 $\blacktriangledown$	11.2 $\blacktriangle$
WiR	61.9	61.6	63.4 $\blacktriangledown$	61.6	61.6	63.9 $\blacktriangledown$	61.6	62.4 $\blacktriangledown$	63.8 $\blacktriangledown$	61.6	62.1 $\blacktriangledown$	62.6 $\blacktriangledown$	72.0 $\blacktriangledown$
WiW	69.1	69.6 $\blacktriangledown$	70.3 $\blacktriangledown$	69.4	69.3	71.1 $\blacktriangledown$	69.3	69.5 $\blacktriangledown$	70.6 $\blacktriangledown$	69.7	68.9 $\blacktriangle$	70.7 $\blacktriangledown$	72.6 $\blacktriangledown$
Yac	0.5	0.4 $\blacktriangle$	0.7 $\blacktriangledown$	0.5	0.4	0.7 $\blacktriangledown$	0.5	0.4	0.6 $\blacktriangledown$	0.5	0.5	0.6 $\blacktriangledown$	0.9 $\blacktriangledown$
B/W	—	3/6	0/10	—	2/2	0/10	—	1/3	0/10	—	1/4	0/10	3/7

The performance of the EAs improves when adopting the IMS. Although not explicitly shown in Table VI, using the IMS is almost always significantly better than using  $p = 1000$ , for all EAs. In particular, the IMS makes the EAs reach bigger population sizes than  $p = 1000$ , as shown in Figure 5 for GP-GOMEA and GP-Trad.

With the IMS, GP-GOMEA becomes preferable to GP-Trad, particularly when the number of subgenerations  $g$  increases. This is linked to the size of populations instantiated by the IMS: the bigger  $g$ , the less runs and the smaller populations at play. Figure 5 shows that GP-Trad tends to reach much bigger population sizes than GP-GOMEA when  $g = 4$  (on average 3 times bigger). This is because GP-Trad executes subgenerations much faster than GP-GOMEA: it does not learn a linkage model, and performs  $p$  evaluations per subgeneration. GP-GOMEA performs  $(2\ell - 2)p$  variation steps (size of LT times population size) and up to  $(2\ell - 2)p$  evaluations per subgeneration (only meaningful variation steps are evaluated).

Note that generating huge populations as done by GP-Trad with  $g = 4$  may be problematic when limited memory is available, especially if caching mechanisms are desirable to reduce the number of expensive evaluations (e.g., caching the output of each node as in [9], [21]).

GP-GOMEA works well with much smaller populations, as long as they are big enough to enable effective linkage learning. Another difference between GP-GOMEA and GP-Trad is that the populations of the former ultimately converge to a same solution, and are terminated, allowing for bigger runs to start. This is unlikely to happen in GP-Trad because of the use of mutation and stochastic (tournament) selection. Consequently, for the larger  $g = 8$ , GP-GOMEA reaches on

average 1.6 times bigger populations than GP-Trad.

As to GP-RDO, it performs poorly on all problems, with all settings. It performs significantly worse than GP-GOMEA on all problems and settings (it is also worse than GP-Trad). This should not come as a surprise: it is known that GP-RDO normally finds big solutions, and also that it needs big solutions to work well, e.g., to build the library of unique subtrees from the population. The strict size limitation basically breaks GP-RDO. However, we remark that this EA was never designed to work under these circumstances. In fact, when solution size is not strictly limited, GP-RDO achieves excellent performance [9].

DTR is compared with GP-GOMEA using the IMS with  $g = 8$ . Although GP-GOMEA is not optimized (e.g., by tuning the function set), it outperforms tuned DTR on 7 out of 10 datasets, often by considerable magnitudes. DTR performs slightly, yet significantly, better on EnC and Tow, and is considerably better than only GP-GOMEA on EnH. Big magnitude differences are likely due to the very different way GP and DTR models are composed.

Test errors and statistical significance are reported in Table VII. Overall, these results are similar to the validation ones, however the difference between GP-GOMEA and GP-Trad is in general less marked (except for  $p = 1000$  where GP-GOMEA is 6 times better than GP-Trad). This can be expected since the solutions returned by the IMS are the best on the validation set, and normally do not generalize as well on the test set. Again, increasing  $g$  makes GP-GOMEA better than GP-Trad, while lowering memory requirements due to smaller populations. GP-RDO remains the worst performing, while the relationship between DTR and GP-GOMEA is essentially the

same as observed on the validation set.

### VIII. DISCUSSION & CONCLUSION

We built upon previous work on model-based GP, in particular on GP-GOMEA, to find accurate solutions with a strict limitation on their size, in the domain of SR. We focused on small solutions, in particular much smaller solutions than typically reported in literature, to prevent solutions becoming too large to be (easily) interpretable, a key reason to justify the use of GP in many practical applications.

A first limitation of this work is that to truly *achieve* interpretability may well require different measures. Interpretation is mostly subjective, and many other factors besides solution size are important, including the intuitiveness of the subfunctions composing the solution, the number of features considered, and the meaning of these features [13], [37]. Nonetheless, much current research on GP for SR is far from delivering any interpretable results precisely because the size of solutions is far too large (see, e.g., [12]).

We considered solution sizes up to  $\ell = 31$  (corresponding to  $h = 4$  for GP-GOMEA with subfunctions of arity  $\leq 2$ ), as interpreting some solutions at this level can already be non-trivial at times. For example, we show the (manually simplified) best test solution found by GP-GOMEA (IMS  $g = 8$ ) for Tower and Yacht, i.e. the biggest and smallest dataset respectively, in Figure 6. The solution for Tower is arguably easier to understand than the one for Yacht.

We believe future work should address the aformentioned limitation: effort should be put towards reaching some form of interpretability notions, that go beyond solution size or other custom metrics (e.g., [42]). User studies involving the end users of the model (e.g., medical doctors for a diagnosis model) could guide the design of notions of interpretability. If an objective that represents interpretability can be defined, the design of multi-objective (model-based) GP algorithms may lead to very interesting results.

Another limitation of this work lies in the fact that we did not study how linkage learning behaves in GP for SR in depth. In fact, it would be interesting to assess when linkage learning is beneficial, and when it is superfluous or harmful. To this end, a regime of experiments where linkage-related outcomes are predefined, such as emergence of specific patterns, needs to be designed. Simple problems where the true function to regress is known may need to be considered. Studies of this kind could provide more insights on how to improve linkage learning in GP for SR (and other learning tasks), and are an interesting direction for future work.

In summary and conclusion, we have identified limits and presented ways to improve a key component of a state-of-the-art model-based EA, i.e. *GP-GOMEA*, to competently deal with realistic SR datasets, when small solutions are desired. This key component is linkage learning. We showed that solely and directly relying on mutual information to identify linkage introduces bias, because the genotype is not uniformly distributed in GP populations, and we provided an approximate normalization method to tackle this problem. We furthermore explored how to incorporate ERCs into linkage learning, and

<b>Tower:</b>
$4668.49 + -3.56((662.77 + x_{21})x_{12} \div_{AQ} x_{15} - x_1 - x_{15} + x_5 + 4x_{12} - x_{23}(x_6 \div_{AQ} x_1 + 1))$
<b>Yacht:</b>
$0.73 + 33004.40(((x_6^2 \div_{AQ} (x_5 x_2)) \div_{AQ} (x_3 x_2 \div_{AQ} (x_2 \div_{AQ} x_1)))(x_6 + 0.30)x_6^5 x_5)$

Figure 6. Examples of best solution found by GP-GOMEA (IMS,  $g = 8$ ).

found that on-line binning of constants is an efficient and effective strategy. Lastly, we introduced a new form of the IMS, to relieve practitioners from setting a population size, and from finding a good generalizing solution. Ultimately, our contributions proved successful in improving the performance of GP-GOMEA, leading to the best overall performance against other EAs, as well as tuned decision trees.

### ACKNOWLEDGEMENT

The authors thank the Foundation Kinderen Kankervrij for financial support (project no. 187), and SURFsara for granting access to the Lisa Compute Cluster.

### REFERENCES

- [1] J. R. Koza, *Genetic Programming: on the programming of computers by means of natural selection*. Cambridge, MA, USA: MIT Press, 1992.
- [2] K. Krawiec, *Behavioral program synthesis with genetic programming*. Springer, 2016, vol. 618.
- [3] J. Zhong, L. Feng, W. Cai, and Y.-S. Ong, “Multifactorial genetic programming for symbolic regression problems,” *IEEE Trans. Syst. Man Cybern. Syst.*, no. 99, pp. 1–14, 2018.
- [4] V. V. De Melo, “Kaizen programming,” in *Genetic and Evolutionary Computation (GECCO 2014)*. ACM, 2014, pp. 895–902.
- [5] J. Źegklitz and P. Pošk, “Symbolic regression algorithms with built-in linear regression,” *arXiv preprint arXiv:1701.03641*, 2017.
- [6] I. Icke and J. C. Bongard, “Improving genetic programming based symbolic regression using deterministic machine learning,” in *IEEE Congr. Evol. Comput. (CEC), 2013*. IEEE, 2013, pp. 1763–1770.
- [7] M. Keijzer, “Improving symbolic regression with interval arithmetic and linear scaling,” in *European Conference on Genetic Programming*. Springer, 2003, pp. 70–82.
- [8] Q. Chen, B. Xue, and M. Zhang, “Generalisation and domain adaptation in gp with gradient descent for symbolic regression,” in *IEEE Congr. Evol. Comput. (CEC), 2015*. IEEE, 2015, pp. 1137–1144.
- [9] T. P. Pawlak, B. Wieloch, and K. Krawiec, “Semantic backpropagation for designing search operators in genetic programming,” *IEEE Trans. Evol. Comput.*, vol. 19, no. 3, pp. 326–340, 2015.
- [10] Q. Chen, B. Xue, and M. Zhang, “Improving generalisation of genetic programming for symbolic regression with angle-driven geometric semantic operators,” *IEEE Trans. Evol. Comput.*, 2018.
- [11] A. Moraglio, K. Krawiec, and C. G. Johnson, “Geometric semantic genetic programming,” in *International Conference on Parallel Problem Solving from Nature*. Springer, 2012, pp. 21–31.
- [12] J. F. B. S. Martins, L. O. V. B. Oliveira, L. F. Miranda, F. Casadei, and G. L. Pappa, “Solving the exponential growth of symbolic regression trees in geometric semantic genetic programming,” in *Genetic and Evolutionary Computation (GECCO 2018)*. New York, NY, USA: ACM, 2018, pp. 1151–1158.
- [13] Z. C. Lipton, “The mythos of model interpretability,” *Queue*, vol. 16, no. 3, pp. 30:31–30:57, Jun. 2018. [Online]. Available: <http://doi.acm.org/10.1145/3236386.3241340>
- [14] P. Orzechowski, W. La Cava, and J. H. Moore, “Where are we now?: A large benchmark study of recent symbolic regression methods,” in *Genetic and Evolutionary Computation (GECCO 2018)*. New York, NY, USA: ACM, 2018, pp. 1183–1190.
- [15] T. Chen and C. Guestrin, “Xgboost: A scalable tree boosting system,” in *Proceedings of the 22nd ACM SIGKDD international conference on knowledge discovery and data mining*. ACM, 2016, pp. 785–794.
- [16] R. Poli, W. B. Langdon, N. F. McPhee, and J. R. Koza, *A field guide to genetic programming*. Lulu. com, 2008.
- [17] D. Thierens and P. A. N. Bosman, “Optimal mixing evolutionary algorithms,” in *Genetic and Evolutionary Computation (GECCO 2011)*. ACM, 2011, pp. 617–624.

- [18] N. H. Luong, H. La Poutré, and P. A. N. Bosman, "Multi-objective gene-pool optimal mixing evolutionary algorithms," in *Genetic and Evolutionary Computation (GECCO 2014)*. ACM, 2014.
- [19] A. Bouter, T. Alderliesten, C. Witteveen, and P. A. N. Bosman, "Exploiting linkage information in real-valued optimization with the real-valued gene-pool optimal mixing evolutionary algorithm," in *Genetic and Evolutionary Computation (GECCO 2017)*. ACM, 2017, pp. 705–712.
- [20] E. Medvet, A. Bartoli, A. De Lorenzo, and F. Tarlao, "Gomge: Gene-pool optimal mixing on grammatical evolution," in *International Conference on Parallel Problem Solving from Nature*. Springer, 2018, pp. 223–235.
- [21] M. Virgolin, T. Alderliesten, C. Witteveen, and P. A. N. Bosman, "Scalable genetic programming by gene-pool optimal mixing and input-space entropy-based building-block learning," in *Genetic and Evolutionary Computation (GECCO 2017)*. New York, NY, USA: ACM, 2017, pp. 1041–1048.
- [22] M. Virgolin, T. Alderliesten, A. Bel, C. Witteveen, and P. A. N. Bosman, "Symbolic regression and feature construction with gp-gomea applied to radiotherapy dose reconstruction of childhood cancer survivors," in *Genetic and Evolutionary Computation (GECCO 2018)*. ACM, 2018, pp. 1395–1402.
- [23] G. R. Harik and F. G. Lobo, "A parameter-less genetic algorithm," in *Genetic and Evolutionary Computation (GECCO 1999)*. Morgan Kaufmann Publishers Inc., 1999, pp. 258–265.
- [24] L. Breiman, *Classification and regression trees*. Routledge, 2017.
- [25] D. Thierens and P. A. N. Bosman, "Hierarchical problem solving with the linkage tree genetic algorithm," in *Genetic and Evolutionary Computation (GECCO 2013)*. ACM, 2013, pp. 877–884.
- [26] I. Gronau and S. Moran, "Optimal implementations of upgma and other common clustering algorithms," *Information Processing Letters*, vol. 104, no. 6, pp. 205–210, 2007.
- [27] M. Ebner, M. Shackleton, and R. Shipman, "How neural networks influence evolvability," *Complexity*, vol. 7, no. 2, pp. 19–33, 2001.
- [28] K. L. Sadowski, P. A. N. Bosman, and D. Thierens, "On the usefulness of linkage processing for solving max-sat," in *Genetic and Evolutionary Computation (GECCO 2013)*. ACM, 2013, pp. 853–860.
- [29] J. Ni, R. H. Drieborg, and P. I. Rockett, "The use of an analytic quotient operator in genetic programming," *IEEE Trans. Evol. Comput.*, vol. 17, no. 1, pp. 146–152, 2013.
- [30] A. Asuncion and D. Newman, "Uci machine learning repository," 2007.
- [31] J. Demšar, "Statistical comparisons of classifiers over multiple data sets," *Journal of Machine learning research*, vol. 7, no. Jan, pp. 1–30, 2006.
- [32] S. Holm, "A simple sequentially rejective multiple test procedure," *Scandinavian journal of statistics*, pp. 65–70, 1979.
- [33] S. Luke and L. Panait, "A survey and comparison of tree generation algorithms," in *Genetic and Evolutionary Computation (GECCO 2001)*. Morgan Kaufmann Publishers Inc., 2001, pp. 81–88.
- [34] E. Medvet, M. Virgolin, M. Castelli, P. A. N. Bosman, I. Gonçalves, and T. Tušar, "Unveiling evolutionary algorithm representation with du maps," *Genetic Programming and Evolvable Machines*, vol. 19, no. 3, pp. 351–389, 2018.
- [35] Y.-J. Lin and T.-L. Yu, "Investigation of the exponential population scheme for genetic algorithms," in *Genetic and Evolutionary Computation (GECCO 2018)*. ACM, 2018, pp. 975–982.
- [36] B. W. Goldman and W. F. Punch, "Parameter-less population pyramid," in *Genetic and Evolutionary Computation (GECCO 2014)*. ACM, 2014, pp. 785–792.
- [37] F. Doshi-Velez and B. Kim, "Towards a rigorous science of interpretable machine learning," *arXiv preprint arXiv:1702.08608*, 2017.
- [38] L. Breiman, "Random forests," *Machine learning*, vol. 45, no. 1, pp. 5–32, 2001.
- [39] C. Gathercole and P. Ross, "An adverse interaction between crossover and restricted tree depth in genetic programming," in *Genetic and Evolutionary Computation (GECCO 1996)*. MIT Press, 1996, pp. 291–296.
- [40] W. B. Langdon and R. Poli, "An analysis of the max problem in genetic programming," *Genetic Programming*, vol. 1, no. 997, pp. 222–230, 1997.
- [41] F. Pedregosa, G. Varoquaux, A. Gramfort, V. Michel, B. Thirion, O. Grisel, M. Blondel, P. Prettenhofer, R. Weiss, V. Dubourg *et al.*, "Scikit-learn: Machine learning in python," *Journal of machine learning research*, vol. 12, no. Oct, pp. 2825–2830, 2011.
- [42] E. J. Vladislavleva, G. F. Smits, and D. Den Hertog, "Order of non-linearity as a complexity measure for models generated by symbolic regression via pareto genetic programming," *IEEE Trans. Evol. Comp.*, vol. 13, no. 2, pp. 333–349, 2009.



**Marco Virgolin** is a PhD candidate at Centrum Wiskunde & Informatica in Amsterdam, the Netherlands, and is enrolled at the Delft University of Technology, Delft, the Netherlands. He holds an M.Sc. in Computer Engineering from the University of Trieste, Italy. Marco is mostly interested in evolutionary and explainable machine learning, with a special focus on genetic programming and symbolic regression. For more information, visit <http://marcovirgolin.github.io>.



**Tanja Alderliesten** received her PhD in computer science in 2004 from the Utrecht University in the Netherlands. Currently, she is a tenured senior researcher at the Department of Radiation Oncology of the Amsterdam UMC, University of Amsterdam, the Netherlands. The focus of her research is translational in nature and primarily concerns the development of state-of-the-art methods and techniques from the fields of mathematics and computer science (including image processing, biomechanical modeling, and optimization) for radiation oncology.



**Cees Witteveen** is a full professor of Algorithmics at Delft University of Technology. The research fields he has been active in include inductive inference, non-monotonic reasoning, logic programming and theory revision. Currently, his research interests concentrate on the design and evaluation of coordination algorithms in distributed systems with self-interested actors especially in planning and scheduling problems. He published more than 150 refereed papers and journal articles in these fields. He is project leader of more than 10 research projects on plan coordination in multi-agent systems, diagnosis, reconfiguration and routeplanning. He is member of the board of the national Dutch AI association, member of the program board of the research school TRAIL, member of the research school SIKS, member of the program board for Computer Science of the Lorentz Center. He was also member of the European Network of Excellence on Planning (PLANET).



**Peter A.N. Bosman** is a senior researcher in the Life Sciences and Health (LSH) research group at the Dutch national research institute for mathematics and computer science (Centrum Wiskunde & Informatica (CWI)) and professor of Evolutionary Algorithms (EAs) at Delft University of Technology. Peter was formerly affiliated with Utrecht University, where he also obtained his M.Sc. and Ph.D. degrees in computer science, both on the design and application of model-based EAs. His research concerns the design of effective and efficient (model-based) EAs as well as their real-world application, primarily in the LSH domain. Peter is best known for his status of active researcher in the EA subfield of Estimation-of-Distribution Algorithms (EDAs) since its upcoming and has (co-)authored over 100 refereed publications, out of which 4 received best paper awards.